From Vaccine to Pathogen: Circulating Vaccine Derived Poliovirus outbreaks require genetic reversion, low immunity, and high exposure doses

Wesley Wong[1*], Jillian Gauld[1*], Michael Famulare[1*]

Author Affiliations

1. Institute for Disease Modeling, Global Good, Intellectual Ventures, Bellevue, WA, USA

* Currently employed at the Bill and Melinda Gates Foundation

Corresponding Author

Michael Famulare

Building IV, 3150 139th Ave SE, Bellevue, WA 98005

+1 (425) 691-3327

mfamulare@idmod.org

Keywords:

Sabin 2, cVDPV2, poliovirus, genetic reversion, evolution, modeling, vaccine

Classification: BIOLOGICAL SCIENCES: Evolution

Author Contributions

WW and MF were involved with model development, analysis, and interpretation. All authors were involved with manuscript writing and interpretation. Correspondence and requests for materials should be addressed to Michael Famulare.

Abstract

The oral poliovirus vaccines (OPV) are one of most effective disease eradication tools in public health. However, the Sabin 2 vaccine strain can revert attenuation and cause outbreaks of circulating, vaccine-derived poliovirus (cVDPV2) that are clinically indistinguishable from wild poliovirus (WPV). Accurately assessing cVDP2 risk requires disentangling the complex interaction between epidemiology and evolutionary biology. Here, we developed a Sabin 2 reversion model that simulates the reversion of Sabin 2 to WPV based on the clinical differences in shedding duration and infectiousness between individuals vaccinated with Sabin 2 and those infected with wild poliovirus. Genetic reversion is informed by a canonical reversion pathway defined by three gatekeeper mutations (A481G, U2909C, and U398C) and the accumulation of genetic load from deleterious nonsynonymous mutations. Our model captures essential aspects of both phenotypic and molecular evolution and simulates transmission using a multiscale transmission model that consolidates the relationships among immunity, susceptibility, and transmission risk. We show that despite the rapid reversion of Sabin 2, cVDPV2 outbreaks can be controlled by maintaining high levels of population-level immunity and sanitation. Supplementary immunization activities must maintain high vaccine coverage to prevent future cVDPV2 outbreaks in the targeted intervention zone, but declining global immunity against Sabin 2 makes them increasingly risky to implement in poor sanitation regions regardless of historical immunization activity. A combined strategy of assessing and improving sanitation levels in conjunction with high coverage vaccination campaigns will limit future cVDPV2 emergence and spread.

Significance Statement

Since the withdrawal of the Sabin 2 oral poliovirus vaccine (OPV2), circulating vaccine-derived poliovirus outbreaks caused by the genetic reversion of Sabin 2 vaccine virus (cVDPV2) have been

increasing in frequency. The current strategies for combating cVDPV2 involve supplemental immunization activities with monovalent Sabin 2 oral poliovirus (mOPV2), which can inadvertently seed future cVDPV2 outbreaks. Accurately assessing future cVDPV2 outbreak risk following mass mOPV2 campaigns is critical poliovirus eradication efforts but must consider the interaction between genetic reversion and epidemiological transmission. We developed an evolutionary epidemiology model to integrate Sabin 2 genetic reversion and transmission into a single framework to evaluate their relative contribution to cVDPV2 outbreaks and inform future intervention strategies.

Introduction

Mass immunization with oral poliovirus vaccine (OPV) has led to a >99.99% drop in wild poliovirus (WPV) cases (1) and the complete eradication of Type 2 and Type 3 WPV. The OPVs are highly efficacious vaccines that confer long-lasting protective immunity (2). A curious feature of these vaccines is that vaccinated individuals can shed and transmit vaccine virus. Vaccine transmission increases population-level immunity but is problematic when viruses revert attenuation, resulting in circulating, vaccine-derived poliovirus (cVDPV) capable of causing paralytic poliomyelitis cases clinically indistinguishable from WPV (3). Following the eradication of Type 2 WPV, the Global Polio Eradication Initiative coordinated the global withdrawal of Sabin 2 OPV (OPV2) from routine immunization schedules (commonly referred to as the Switch) to prevent future sources of circulating, vaccine-derived Type 2 poliovirus (cVDPV2) (1).

Despite the Switch, cVDPV2 outbreaks continue to be a pressing public health concern and have emerged as a significant issue threatening global poliovirus eradication efforts (1, 4). Although OPV2 is no longer used in routine immunization, monovalent OPV2 (mOPV2) vaccination campaigns are still used as supplemental immunization activities (SIAs) to combat cVDPV2 outbreaks. cVDPV2 outbreaks

69 are now reported throughout the African continent, Pakistan, Afghanistan, China, Malaysia and the
70 Philippines and 29% of the outbreaks in Africa have involved international spread (4, 5). Since the
71 Switch, 126 mOPV2 campaigns utilizing more than 300 million doses of OPV2 have been implemented to
72 control cVDPV2 outbreaks (6). These SIAs are estimated to be responsible for seeding over half of the
73 cVDPV2 outbreaks observed since the Switch (6). Ensuring the future safety and efficacy of these SIA
74 campaigns while minimizing the risk of seeding future cVDPV2 outbreaks is critical to the success of the
75 poliovirus eradication initiative.

76 The Sabin 2 vaccine strain was derived from a wild-type isolate (P22/P712/56) passaged in
77 monkey kidney cells to achieve neurovirulence attenuation (7). However, identifying the genetic
78 mutations responsible for attenuation has been surprisingly complicated, in part because the progenitor
79 has not been fully sequenced and because P22/P712/56 is thought to be naturally attenuated relative to
80 other WPV strains (8). Despite this, phylogenetic analyses of whole genome sequences collected from
81 cVDPV2 outbreaks suggest a common evolutionary pathway to attenuation reversal (9). This pathway is
82 characterized by the rapid fixation three gatekeeper mutations, A481G, U2909C, and U398C, within the
83 first few weeks after vaccination (9, 10). All three mutations have previously been implicated as
84 molecular determinants of attenuation for Sabin 2 (11–14). A481G and U398C are noncoding mutations
85 that affect the stability of a 5' hairpin structure that mediates translation efficiency (13, 15, 16) and
86 U2909C is a nonsynonymous mutation in the VP1 capsid protein.

87 However, genetic reversion is not the sole determinant of cVDPV2 emergence, which we
88 generally define as an outbreak of vaccine-derived paralytic poliomyelitis cases large enough to be of
89 public health concern. Environmental sewer samples have identified revertant strains in regions with no
90 detectable cVDPV2 cases (17). In fact, vaccinated individuals can shed and transmit revertant viruses to
91 other individuals (10, 18), but whether this results in clinically-detected cVDPV2 outbreaks strongly
92 depends on the epidemiological context. These cVDPV2 outbreaks are associated with regions with

93 historically poor vaccination rates and low population-level immunity (6, 19). Thus, while Sabin 2
94 reversion is a prerequisite of cVDPV2 emergence, whether it is transmitted frequently enough to trigger
95 a public health crisis depends on the interactions between genetic reversion and local epidemiological
96 conditions.

97 Mathematical models can be useful tools for assessing cVDPV2 emergence risk and
98 characterizing the evolutionary and epidemiological factors that allow cVDPV2 outbreaks to occur. We
99 developed an evolutionary-epidemiology model that simulates Sabin 2 reversion as it is transmitted in
100 an epidemiological model previously calibrated during an mOPV2 clinical trial performed in Matlab,
101 Bangladesh (20). The combined model allows us to assess the consequences of vaccine reversion in the
102 context of an actual epidemiological setting. By unifying evolutionary theory, population genetics, and
103 epidemiology into a single framework, our study provides a holistic understanding of cVDPV2
104 emergence as it relates to both genetic reversion and transmission.

105

106 **Results**

107 *Brief model structure overview*

108 We previously developed agent-based multiscale epidemiology model designed to replicate
109 household community structure and Sabin 2 vaccine transmission during an mOPV2 clinical trial
110 performed in Matlab, Bangladesh (20, 21). Transmission is contact based and made heterogeneously
111 depending on household community structure membership (**Figure 1A**). Susceptibility is defined by a
112 dose-response model that determines the probability of infection given the strain-specific viral
113 infectiousness, the total viral exposure dose per contact, and the immunity of the recipient host. The
114 total viral exposure dose is determined by the viral shedding concentration of the infected individual
115 and the average fecal-oral dose per contact in the population. Immunity is defined by the OPV-

116 equivalent antibody titer that determines infection probability. Individuals with low immunity upon
117 infection have longer shedding durations and higher viral shedding titers. Further details of the
118 epidemiology model are described elsewhere (21, 22).

119 Here, we developed and integrated a new Sabin 2 reversion model into the multiscale
120 epidemiology model. Sabin 2 evolution is modeled as a population of multiple viral lineages founded by
121 a Sabin 2 vaccine virus strain during vaccination. These viral lineages evolve independently and compete
122 for the limited availability of naïve or low-immunity individuals in the population. Phenotypic evolution
123 is driven by the reversion of three gatekeeper mutations (A481G, U2909C, and U398C) and the
124 accumulation of deleterious nonsynonymous mutations generated through mutation and purged
125 through selection or genetic drift (**Figure 1B**). We assume complete genetic reversion results in a viral
126 population whose average infectiousness and shedding duration is identical to those of WPV. Due to the
127 independent acquisition of mutations across different viruses and viral lineages, individual viruses have
128 different infectiousness and shedding duration phenotypes even after the three gatekeeper mutations
129 have reverted.

130 *Simulating Sabin 2 molecular evolution*

131 To inform molecular evolution, intra-host substitution rates for the three gatekeeper mutations
132 were based on estimates previously calculated from 241 Vp1 (viral protein 1) segments from Sabin-like
133 poliovirus collected during routine surveillance in Nigeria (10, 23). Nonsynonymous and synonymous
134 substitution rates were calibrated (**SI Appendix**) to a set of whole genome sequences and VP1 capsids
135 segments isolated from infections from confirmed Sabin 2, Sabin-like, vaccine-derived poliovirus (VDPV)
136 and cVDPV2 cases (**Figure 2**). One notable feature of poliovirus evolution is the discordance between
137 short-term evolution following vaccination and long-term evolution after prolonged circulation. Short-
138 term evolution is dominated by the accumulation of nonsynonymous mutations, as evidenced by the

139 increased rate of nonsynonymous mutation accumulation in the whole genome sequences during the
140 first year of evolution (**Figure 2B**), the reduction in the ratio of nonsynonymous to synonymous
141 mutations over time (**Figure 2D**), and the elevated dN/dS ratios of Sabin-like samples compared to
142 cVDPV2 samples (**Supplemental Figure 1**).

143 We hypothesized that the difference between short-term and long-term evolution represents a
144 shift in the distribution of fitness effects for nonsynonymous mutations. Simulated nonsynonymous
145 mutations were divided into two categories: deleterious mutations that can cause a reduction in either
146 infectiousness or shedding duration, and neutral mutations that have no phenotypic effect. Each
147 category is associated with a different substitution rate and deleterious nonsynonymous mutations are
148 purged using a recombination-like process that mimics selection and intra-species recombination within
149 the host (**SI Appendix**). Deleterious nonsynonymous mutations dominate molecular evolution during the
150 first year of evolution while neutral nonsynonymous mutations dominate molecular evolution after
151 prolonged circulation (**Figure 2E**).

152 *Simulating Sabin 2 reversion*

153 Genotype-to-phenotype maps for shedding duration were generated by comparing the
154 shedding duration of naïve individuals vaccinated with Sabin 2 (median 30.3, average 36 days) with
155 those infected with WPV (median 40.3, average 48 days) (**SI Appendix**). Due to the rapid intra-host
156 fixation of the three gatekeeper mutations (**Figure 3A**), we assert that reversion during an infection
157 extends its shedding duration (**Figure 3B**). Prior to any intra-host evolution, the genotype-to-phenotype
158 map for shedding duration estimates that naïve individuals vaccinated with non-reverted Sabin 2 have a
159 median shedding duration of 13.5 days (**Figure 3B**, *dashed red line*). The clinically-observed shedding
160 durations of Sabin 2 vaccinated individuals (**Figure 3B,** *solid red line*) is realized as the average shedding
161 durations of different viral genotypes composed of unmutated and reverted Sabin 2 viruses

162 (**Supplemental Table 1**). After vaccination, 7.6% of simulated vaccinated individuals shed non-reverted
163 Sabin 2 at the end of shedding, 92.4% shed virus with at least one reverted gatekeeper mutation, and
164 35.2% shed virus with all three gatekeeper mutations reverted. Interestingly, we did not identify a
165 deleterious cost (reduction in shedding duration) associated with nonsynonymous mutation
166 accumulation (**SI Appendix**).

167 The genotype-to-phenotype map describing viral infectiousness was based on clinical
168 differences of human dose response between Sabin 2 and WPV. Unlike shedding duration, we identified
169 a small negative effect associated with deleterious nonsynonymous mutations resulting in a reduction in
170 viral infectiousness (**SI Appendix**). Our model predicts that viral genotypes with no deleterious
171 nonsynonymous mutations but are reverted at A481G and U2909C are more infectious than typical WPV
172 strains (**Figure 3C**). Each additional deleterious nonsynonymous mutation reduces infectiousness such
173 that a viral genotype with all three gatekeeper mutations reverted and nine deleterious mutations is as
174 infectious as WPV (**Figure 3D**).

175

176 *Examining the evolutionary epidemiology dynamics of Sabin 2 reversion*

177 To explore how Sabin 2 reversion and transmission interact, we simulated transmission
178 following an mOPV2 campaign targeting 10% of children under five in a population with 10 times the
179 fecal-oral dose of Matlab (2.5e-6 grams per contact) five years after vaccination cessation (**Figure 4**).
180 These epidemics are cyclic (**Figure 4A**) and characterized by boom-bust cycles that eventually stabilize
181 within the first three years of transmission. Under these conditions, 10% of stochastic replicates failed to
182 establish stable, endemic transmission. These stochastic replicates failed after the initial expansion wave
183 collapsed (**Supplemental Figure 2A**). Should transmission recover, the epidemic rebounds and the
184 proportion of individuals with no immunity (serum neutralizing antibody titer < 8) declines while the

185 proportion of individuals with high immunity (serum neutralizing antibody titer > 256) increases (**Figure**
186 **4B**). Towards the end of the initial epidemic, the proportion of individuals with no immunity begin to
187 increase due to a combination of new births and the waning of pre-existing immunity and sets up the
188 conditions for the next wave of infections.

189 Complete Sabin 2 reversion (**Figure 4C-D**) occurred within the first 200 days of transmission. To
190 describe the evolutionary dynamics of the simulated viral population, we focused on the expected mean
191 (the average of the average) phenotype and the variance of the expected mean. While both shedding
192 duration and infectiousness converged to the WPV phenotype, shedding duration approached it
193 monotonically while infectiousness exceeded WPV during the first few months of transmission. The
194 expected means of both phenotypes were not sensitive to changes in infection number. However, the
195 variance of the expected mean fluctuated over time and was sensitive to epidemiological dynamics. This
196 variance was smallest at the onset of the epidemic when infection numbers were highest and biggest
197 around day 400 when infection number was the smallest. The variance of the expected mean was
198 inversely correlated with total infection number, but its magnitude also depended on the rate with
199 which the epidemic was increasing or decreasing over time (**Figure 4, Supplemental Figure 3**).

200 Surprisingly, complete Sabin 2 reversion does not guarantee stable transmission. The
201 simulations with observed transmission failure did not show a lack of evolutionary fitness: the simulated
202 viral populations in these simulations had infectiousness and shedding durations equivalent to or
203 exceeding that of WPV (**Supplemental Figure 2B-C**).

204 *Population-level immunity and hygiene are major constraints of cVDPV2 emergence*

205 We next utilized this model to simulate cVDPV2 emergence and understand risk. Our scenarios
206 included a point importation of an infant vaccinated with Sabin 2, and a mass vaccination campaign with
207 up to 80% coverage in children under five years of age. We explored scenarios with fecal oral doses

208 equal to, five times greater, and 10 times greater than Matlab (**Figure 5**). The fecal oral dose, combined
209 with the infection-specific, time-dependent viral shedding concentration per gram of stool (22),
210 determines the total exposure dose per infectious contact. cVDPV2 emergence was defined as an
211 outbreak significant enough to trigger a warning from passive routine surveillance efforts. However,
212 because surveillance is not currently simulated, we operationally define cVDPV2 emergence as a
213 simulation with sustained cVDPV2 transmission for at least three years.

214 We found zero risk of cVDPV2 emergence following a mass vaccination campaign (**Figure 5A**) or
215 point importation event (**Figure 5D**) in Matlab with its current fecal oral dose. However, cVDPV2
216 emergence is possible at higher fecal-oral doses. Under these conditions, cVDPV2 emergence risk
217 increases with time since vaccination, but is controlled within the community by higher vaccination
218 coverage. When the fecal-oral dose was five times that of Matlab (1.8e-6 grams per contact), all
219 vaccination campaigns and point importations immediately after vaccination cessation (year 0) had a
220 less than 0.05 chance of causing a cVDPV2 emergence (**Figure 5B**). Vaccination campaigns with less than
221 30% coverage in populations with more than three years of vaccination cessation had the highest risk of
222 cVDPV2 emergence, with an emergence rate between 20% and 30%. Following point importation,
223 cVDPV2 emergence risk rises from 0% immediately after cessation to 20% after five years of cessation
224 (**Figure 5E**).

225 When the fecal-oral dose was ten times that of Matlab (2.5e-6 grams per contact), high
226 vaccination coverage could not efficiently prevent cVDPV2 emergence (**Figure 5C**). Immediately after
227 vaccination cessation, simulations with high vaccination coverage (> 70% coverage) resulted in cVDPV2
228 emergence 40-50% of the time. All other scenarios had a greater than 60% chance of cVDPV2
229 emergence. This increases to a greater than 80% chance following a vaccination campaign with less than
230 30% coverage in populations with more than three years of vaccination cessation. cVDPV2 emergence

231 risk following a point importation event increases sharply with time since vaccination (**Figure 5F**),
232 increasing from 5% immediately after cessation to 55% after five years of cessation.

233

234 **Discussion**

235 cVDPV2 outbreaks are serious public health dilemmas made possible by viral evolution and
236 exacerbated by epidemiological conditions. By unifying evolutionary and epidemiological theory into a
237 single framework, our model assesses cVDPV2 emergence risk in relation to changes in shedding
238 duration and infectiousness associated with vaccine reversion and the constraints to transmission
239 imposed by immunity, sanitation, and contact structure. To overcome the lack of direct transmission
240 measurements for Sabin 2 reversion intermediates, we generated genotype-to-phenotype maps for
241 shedding duration and viral infectiousness by relying on established molecular evolution and population
242 genetic theory.

243 Sabin 2 reversion can be viewed as an adaptive process where Sabin 2 must climb up a fitness
244 landscape to achieve the optimal, WPV-like phenotype. Within the poliovirus virology literature, Sabin 2
245 is commonly presented as a purely adaptive process where fixed mutations contribute positively to the
246 emergence of the WPV phenotype (24). However, it is unlikely that all fixed nonsynonymous mutations
247 are beneficial (25) and viruses must purge deleterious mutations to prevent Muller's Ratchet from
248 causing an irreversible decline in viral fitness (26, 27). Muller's ratchet can be avoided by engaging in
249 intra-species or inter-species recombination with Enterovirus C viruses (28) and by altering the
250 distribution of fitness effects (DOFE) for fixed mutations (29, 30). The latter is based on Fisher's
251 Geometric Model (FGM) of adaptive evolution, which predicts that mutations with large-phenotypic
252 effects are unlikely to fixate the closer an organism is to its fitness optimum. Our model incorporates
253 FGM by attributing large phenotypic effects to the gatekeeper mutations and specifying

254 nonsynonymous mutation rates so that early adaptive evolution is dominated by deleterious
255 nonsynonymous mutations while long-term evolution is dominated by neutral ones.

256 Interestingly, we failed to identify a deleterious cost associated with nonsynonymous mutations
257 and shedding duration but did identify one associated with nonsynonymous mutations and infectivity.
258 This finding suggests that there are differences between intra-host and inter-host selection. This could
259 reflect strong purifying selection induced by the highly competitive intra-host survival dynamics due to
260 high viral titers. Conversely, the deleterious cost associated with infectiousness could result from the
261 genetic drift induced by the severe sampling of viral genotypes during person-to-person transmission
262 (25, 31). Strong genetic drift could weaken the efficacy of purifying selection in removing deleterious
263 mutations associated with inter-host transmission, but more work is needed to assess differences in
264 inter- and intra-host selection. The phenotypes we modeled are the consolidation of multiple factors
265 such as cell invasion, replication, immune evasion, and environmental survival. These subfactors likely
266 contribute to both shedding duration and infectiousness, but our ability to map molecular evolution to
267 these subfactors remains limited.

268 At its core, cVDPV2 emergence is an evolutionary and epidemiological problem that requires a
269 combined approach to properly assess how the two interact. From an evolutionary perspective, the
270 availability of susceptible hosts and the distribution of transmissions dictates the strength of genetic
271 drift. Once the gatekeeper mutations are fixed, the phenotypic stability of the viral population is
272 maintained as a mutation-selection-drift balance and the range of phenotypic values explored by the
273 viral population is determined by the total number of infected individuals in the population. From an
274 epidemiological perspective, Sabin 2 reversion causes infectiousness and shedding duration to rapidly
275 increase within the first 200 days of vaccination and allow more individuals to become infected. Despite
276 the emergence of WPV-like viruses in our simulations, complete genetic reversion of Sabin 2 does not
277 guarantee a cVDPV2 outbreak. Whether these viruses cause a cVDPV2 outbreak requiring public health

278 intervention depends on population-level immunity and the average viral exposure dose per infectious
279 contact (4, 6, 22, 32).

280 The current strategies for controlling cVDPV2 involve implementing aggressive mOPV2 SIA
281 activities in outbreak response zones and neighboring regions, intensifying routine immunization in
282 high-risk areas with inactivated polio vaccine (IPV), ensuring a sufficient supply of Sabin 2 OPV for future
283 eradication strategies, and identifying high cVDPV2 outbreak risk zones (33). Our work clearly shows
284 that even regions with historically high vaccination rates are prone to cVDPV2 outbreaks if sanitation is
285 poor. Evaluations of high cVDPV2 outbreak risk regions should include sanitation assessments and utilize
286 tools designed to measure fecal contamination for other fecal-oral pathogens such as *E. coli* (34). Prior
287 to mass immunization with OPV2, sanitation assessments should be made to assess the risk of a cVDPV2
288 outbreak in both the targeted intervention zone and in the surrounding regions. These assessments will
289 be useful for resource allocation and for determining the minimum coverage needed to prevent future
290 cVDPV2 outbreaks. Regions with poor sanitation will require aggressive, high-coverage SIA vaccination
291 campaigns to prevent seeding future cVDPV2 outbreaks.

292 Sanitation assessments will also help public health officials determine whether additional WASH
293 (water, sanitation, and hygiene) interventions are needed to supplement ongoing vaccination activity.
294 Our study reconfirms that there are sanitation regimes defined by high fecal oral doses that is
295 guaranteed to seed future cVDPV2 outbreaks (22), regardless of vaccination coverage. Although long-
296 term investments in infrastructure are prohibitively expensive, relatively simple measures such as the
297 installation of sanitary latrines and drinking water tubewells have been effective at reducing fecal
298 contamination in Matlab, Bangladesh (35). Optimistically, short-term sanitation interventions may be
299 effective if implemented similarly to an emergency response campaign (36), especially if they are
300 targeted at vaccine recipients and their immediate household community members (21).These targeted,
301 short-term sanitation interventions could alleviate some of the challenges associated with non-

302 compliance, long-term adherence failure, and poor implementation that reduce the efficacy of standard
303 WASH interventions (37, 38).

304 Our model lays the foundations for integrating population genetic theory and epidemiology to
305 study the evolutionary epidemiology dynamics of rapidly evolving infectious diseases. The success of our
306 framework hinges on an understanding of a pathogen's evolutionary trajectory as well as the initial and
307 ending phenotypic states. We anticipate our model will be extended to the novel OPV2 (nOPV2)
308 candidates (39) as more about their clinical phenotypes and molecular evolution are known. Depending
309 on how attenuated and evolutionarily stable the novel OPV2 candidates are relative to Sabin 2, mass
310 nOPV2 vaccination may reduce the need to also control sanitation levels. We also anticipate our model
311 will be useful for assessing the risks associated with the live-attenuated varicella zoster vaccines, which
312 also shows strong evidence of attenuation reversion conferred by a commonly accessed evolutionary
313 pathway (40).

314 **Materials and Methods**

315 **Sequencing Data**

316 We downloaded fasta files for the VP1 segments and whole genome sequences of Sabin 2 and
317 Sabin 2 derived genomes from Genbank. These samples were collected across 102 studies performed in
318 countries including Egypt, Madagascar, China, Nigeria, the United States, Israel, Switzerland, and the
319 Democratic Republic of Congo. Multiple sequence alignments were first generated using MUSCLE
320 (v3.8.31) (41). Sequences were compared to a known Sabin 2 sample (accession ID: AY184220) to
321 identify and remove insertions. Sequences with long internal gaps (>15 bases) and coverage < 30%
322 (percentage of called bases) were discarded. Coding sequence alignments from the whole genome
323 sequences were generated for each of the poliovirus coding regions by generating multiple sequence

324 alignments for each of the 15 translated protein coding sequences of the poliovirus genome. These
325 alignments were further filtered to remove samples with < 90% coverage.

326 A total of 177 whole genome sequences and 1,643 VP1 sequences were retained for analysis.
327 Samples were classified as Sabin 2, Sabin-Like, VDPV (vaccine-derived poliovirus), iVDPV
328 (immunodeficiency-related vaccine-derived poliovirus), cVDPV2 based on their original study
329 classifications. Viruses that displayed <1% VP1 nucleotide sequence difference from the parental Sabin 2
330 genome were classified as Sabin-lik2 and those with 1-15% nucleotide sequence difference were
331 classified as VDPV. VDVPVs isolated from immunodeficient individuals were classified as iVDPV while
332 samples with evidence of having originated from prior transmission are classified as cVDPV2. The whole
333 genome sample set also included the Lansing and MEF-1 laboratory strains as well as several engineered
334 Lansing strain derivatives. Accession numbers, classifications, and study origin for each sample are in
335 **Supplemental File 1** and **Supplemental File 2**. FASTA files for the aligned VP1 and whole genome coding
336 sequences are available on the **Github repository.**

337 Coding sequence alignments were used to generate a phylogenetic tree using RAxML (v8.2.10)
338 with a general time reversable CAT (GTRCAT) model (42). Estimates of nonsynonymous and synonymous
339 mutation counts and dN/dS were based off the RAxML generated phylogenetic tree. Estimates of
340 nonsynonymous and synonymous mutation counts from the VP1 sequences were counted directly from
341 the sequence data. Nonsynonymous and synonymous mutation counts for codons with multiple
342 mutations were averaged across all possible, unweighted evolutionary paths.

343 **Model Description**

344 *Defining Genotypes*

345 Genotypes are defined relative to the Sabin-2 genome and defined by the reversion state of
346 three gatekeeper mutations (A481G, U2909C, and U398C), and the number of newly derived

347 nonsynonymous and synonymous mutations in the rest of the genome. The Sabin-2 genome is defined
348 as an array with 6 different mutation classes:

$$G_{S2} = [0, 0, 0, 0, 0, 0]$$

349 The first three are Boolean flags that indicate the allelic states of A481G, U2909C, and U398C (0 =
350 unreverted, 1 = reverted). The last three elements represent the total number of deleterious
351 nonsynonymous, neutral nonsynonymous, and synonymous mutations present in the genome. The
352 counts in the latter categories exclude the three gatekeeper mutations. Splitting nonsynonymous
353 mutations into neutral and deleterious simplifies the true distribution of fitness effects and was
354 necessary to reconcile phenotypic and molecular evolution (**SI Appendix**). These genotypes represent
355 the consensus sequence of fixed variants within vaccinated and infected individuals.

356 For evolved poliovirus strains, we use the notation:

$$G_{i,j,k,nonsyn_{del},nonsyn_{neutral},syn}$$

357

358 where *i*, *j*, and *k* are replaced with the allelic states of A481G, U209C, and U398C. $nonsyn_{neutral}$,
359 $nonsyn_{del}$, and syn are replaced with their respective counts or replaced with X if these mutation
360 classes are irrelevant. For example, $G_{0,0,0,0,0,0}$ is equivalent to the unmutated Sabin-2 vaccine strain (G_{S2})
361 and $G_{1,1,1,10,2,15}$ is a genotype where all three gatekeeper mutations have reverted and where 10
362 deleterious nonsynonymous, 2 neutral nonsynonymous, and 15 synonymous mutations have
363 accumulated.

364 *Genomic evolution: Modeling Sabin 2 molecular evolution*

365 Genomic evolution is modeled using intra-host substitution rates (λ), the fixation of newly
366 derived mutations within the host, for each mutation class (λ_{A481G}, λ_{U2909C}, λ_{U398C}, λ_{syn},
367 $\lambda_{nonsyn,del}$, $\lambda_{nonsyn,neutral}$). This substitution rate reflects the true de novo mutation rate, genetic drift,
368 and selection within the host. This simplification allows us to use a single consensus genome to
369 represent the fixed mutations present in the intra-host viral population. Each mutation class (the three
370 gatekeeper mutations, synonymous mutations, deleterious nonsynonymous mutations, and neutral
371 nonsynonymous mutations) is associated with a substitution rate that describes its expected fixation
372 time (**Supplemental File 3**).

373 To accommodate the effects of intra-host competition and recombination, deleterious
374 nonsynonymous mutation accumulation also depends on a recombination-like mechanism with rate
375 $\lambda_{recombination}$ that purges deleterious mutations from the genome (26, 28, 43). Intra-host substitution
376 rates for the gatekeeper mutations were used as described in (10) while λ_{syn},
377 $\lambda_{nonsyn,del}$, $\lambda_{nonsyn,neutral}$, and $\lambda_{recombination}$ were calibrated to the whole genome sequences and
378 VP1 segments downloaded from Genbank. Only confirmed Sabin 2, Sabin-Like, VDPV, and cVDPV
379 samples were used for calibration. All other samples were excluded from calibration. Calibration details
380 are provided in the **SI Appendix**.

381 Upon vaccination with Sabin 2, fixation times for all mutation classes are calculated by drawing
382 from exponential distributions whose rate parameters are defined by the substitution rate of each
383 mutation class. For the three gatekeeper mutations, these fixation times determine the time to
384 reversion. For nonsynonymous and synonymous mutations, these fixation times determine the time to
385 the next substitution event. To prevent Mueller's Ratchet from resulting in infinite deleterious mutation
386 load, we also draw a time to the next "recombination" event from an exponential distribution defined
387 by $\lambda_{recombination}$. During each "recombination" event, the model draws a random number from a

388 discrete, uniform distribution ranging from zero to $n_{nonsyn,deleterious}$, the number of deleterious
389 nonsynonymous mutations in the genome, to determine the number of deleterious mutations to
390 remove. Conceptually, this represents purifying selection within the host and allows us to accommodate
391 the assumed increase in purifying selection as Sabin 2 reverts to cVDPV2. Pseudocode is provided in
392 ***Supplemental Figure 4***.

393

394 *Genotype to Phenotype: Mapping molecular genetics to shedding duration and infectiousness*

395 A core assumption of our model is that each of the three gatekeeper mutations contributes to
396 the final, WPV phenotype proportional to their relative substitution rates. This assumption is based in
397 part on evolutionary fitness landscape and adaptation theory, which posits that beneficial mutations of
398 large effect are more likely to be fixed early on when an organism is far the optimal fitness peak on a
399 simple, non-rugged fitness landscape (29, 44). By definition, attenuated Sabin 2 vaccine strains are far
400 from the optimal fitness peak for human infection and genetic reversion is the process of climbing the
401 fitness landscape to reach the optimal, WPV-like phenotype. Because of their fast substitution rate, we
402 attribute the bulk of phenotypic change to A481G, followed by U2909C, and to a lesser extent U398C.
403 The ranked ordering of phenotypic effect in our model is supported in the literature. A481G and U2909C
404 are consistently identified as the primary molecular determinants of reversion in *in vitro* and *in vivo*
405 studies (11–16). U398C is only occasionally identified by these studies but its recurrent fixation within
406 the first few months of transmission (9, 10) suggest its adaptive benefit may be too small to be assessed
407 in laboratory-based assays relative to A481G and U2909C.

408 Two epidemiologically relevant phenotypes were calculated for each infection based on its
409 corresponding genotype: 1) shedding duration and 2) infectiousness. Both shedding duration and
410 infectiousness are based on a previously described poliovirus dose-response model (22). Conceptually,

411 the shedding duration is analogous to intra-host selection and infectiousness is analogous to inter-host

412 selection. Details regarding model calibration are deferred to the **SI Appendix**.

413 We assume shedding duration follows a log-normal survival distribution with the form:

$$P\left(shedding\ at\ \mathrm{t}\,\middle|N_{ab_{pre}}; infected\ at\ t = 0\right) \tag{1}$$

$$= \frac{1}{2}\left(1 - erf\left(\frac{ln(t)\ -\ (\mathrm{M_g}\ - \log(\delta)\log_2(N_{ab_{pre}})}{\sqrt{2}ln(\mathrm{S_g})}\right)\right)$$

414 where $N_{ab_{pre}}$ is the pre-infection OPV-equivalent antibody titer (22). For each genotype, $\mathrm{M_g}$ and S_g are

415 genome-specific parameters that influence the average shedding duration and its standard deviation.

416 The mean of this log-normal distribution is defined by $\mathrm{M_g}\ - \log(\delta)\log_2(N_{ab_{pre}})$ and its standard

417 deviation defined by $\mathrm{S_g}$.

$$M_g = \log(\mu_{S2}) + w_{shedding,g} \tag{2}$$

418

$$S_g = \sigma\sqrt{|1 + w_{shedding,g}|} \tag{3}$$

419

$$w_{shedding,g} = 0 + s_{dur,A481G} * G_{A481G} + s_{dur,U2909C} * G_{U2909C} + s_{dur,U398C} * G_{U398C} + s_{dur,nonsyn_{del}} * n_{nonsyn_{del}} \tag{4}$$

420

421 where μ_{S2} is the average shedding duration of a completely unevolved Sabin 2 virus (G_{S2}) in

422 immunologically naiive individuals ($N_{ab_{pre}} = 1$), σ the standard deviation in shedding duration for G_{S2}.

423 $w_{shedding,g}$ defines the shedding duration fitness of a strain, G_{A481G}, G_{U2909C}, and G_{U398C} refer to the

424 allelic status of the three gatekeeper mutations, and $s_{dur,A481G}$, $s_{dur,U2909C}$, $s_{dur,U398C}$ are selection
425 coefficients that describe the change in shedding duration conferred by each of these mutations. Note
426 that fitness is additive but in log space.

427 Upon infection or vaccination, we randomly draw a shedding duration from a lognormal
428 distribution with mean $\mathrm{M_g} - \log(\delta)\log_2(N_{ab_{pre}})$ and standard deviation $\mathrm{S_g}$. A core feature of our
429 shedding duration model is that new gatekeeper mutations arising within the host extends shedding
430 duration. If a new gatekeeper mutation is acquired, the shedding duration is extended:

$$Duration = Duration_{initial} * e^{S_{gateway} + Norm(0,\sigma)\sqrt{S_{gateway}}} \quad (5)$$

431

$$S_{gateway} \in \{s_{dur,A481G}, s_{dur,U2909C}, s_{dur,U398C}\} \quad (6)$$

432

433 where $D_{initial}$ is the shedding duration before acquisition of the gatekeeper mutation and $S_{gateway}$ is
434 the shedding duration selection coefficient for the gatekeeper mutation. Note that $Duration_{initial}$ and
435 the increase in shedding duration, $e^{S_{gateway} + Norm(0,\sigma)\sqrt{S_{gateway}}}$, are log-normally distributed and that
436 multiplying two, independent log-normal distributions results in a log-normal distribution whose mean
437 and variance are the sum of the mean and variances of the original distributions. As a result, shedding
438 duration is the summation of multiple, genome-specific shedding durations whose weights are time-
439 dependent and depend on the fixation of A481G, U2909C, U398C and the accumulation of
440 nonsynonymous mutations.

441 Infectiousness is defined by a beta-Poisson model that assumes a single infectious unit is
442 sufficient to start an infection and that multiple infectious units contribute independently to the
443 probability of infection:

$$P(infection|dose, N_{ab}) = 1 - \left(1 + \frac{dose}{\beta_g}\right)^{-\alpha(N_{ab})^{-\gamma}} \quad (7)$$

444

445 where α and β_g are parameters for a beta-Poisson function, dose is the viral exposure dose, and γ
446 captures the reduction in shedding probability with increasing immunity. Altering the β parameter
447 shifts the beta-poisson function along the x-axis (dose) and altering the α parameter changes its slope.
448 Differences in infectiousness between Sabin 2 strains and WPV can be modeled using the same α but
449 with modified β parameters (22). We interpret the β parameter as a measurement of strain infectivity
450 and define β_g as:

451

$$\beta_g = \frac{\beta}{\left(1 + s_{inf,A481G}\right)^{G_{A481G}} \left(1 + s_{inf,U2909C}\right)^{G_{U2909C}} \left(1 + s_{inf,U398C}\right)^{G_{U398C}} \left(1 + s_{inf,nonsyn_{del}}\right)^{n_{nonsyn_{del}}}} \quad (8)$$

452

453

454 where β is the strain infectivity parameter for Sabin 2 (22) (assuming no evolution), $s_{inf,A481G}$,
455 $s_{inf,U2909C}$, $s_{inf,U398C}$, $s_{inf,nonsyn_{del}}$ are selection coefficients denoting the change in infectiousness
456 conferred by each of the gatekeeper mutations, and $n_{nonsyn_{del}}$ are the number of nonsynonymous
457 mutations in the genome. Parameter estimates were obtained by comparing the CCID50 between Sabin
458 2 and WPV (**SI Appendix**). The inferred selection coefficients for the three gatekeeper mutations are
459 positive (increases infectiousness) while the selection coefficient for deleterious nonsynonymous
460 mutations was negative (decreases infectiousness). Infectiousness is calculated only at the onset of
461 either vaccination or infection.

462

463 **Acknowledgements**

464 We acknowledge all members of the Institute for Disease Modeling, Global Good, and the Bill and
465 Melinda Gates Foundation for their useful discussion and input. We also acknowledge Adam Lauring and
466 Andrew Valesano for early manuscript edits and comments.

467 **Funding**

468 Funding was provided by Bill and Melinda Gates through the Global Good Fund. Funders had no role in
469 the study design, data collection, analysis, interpretation, or writing of the manuscript. The
470 corresponding author had full access to all the data in our study and had final responsibility for the
471 decision to submit for publication.

472 **Data Availability**

473 Data and code will be made publicly available at
474 https://github.com/InstituteforDiseaseModeling/MultiscaleModeling/tree/evo_epistasis upon
475 publication.

476 **Declaration of Interests**

477 The authors declare no competing interests during the study. WW, JG, and MF were employed by the
478 funders through the Bill and Melinda Gates Foundation after study completion.

479 **References**

480 1. F. Khan, *et al.*, rogress Toward Polio Eradication — Worldwide, January 2016–March 2018.
481 *MMWR Morb Mortal Wkly Rep 2019*, 524–528 (2018).

482 2. A. S. Bandyopadhyay, J. Garon, K. Seib, W. A. Orenstein, Polio vaccination: past, present and
483 future. *Future Microbiol.* **10**, 791–808 (2015).

484 3. H. E. Jenkins, *et al.*, Implications of a Circulating Vaccine-Derived Poliovirus in Nigeria. *N. Engl. J.*
485 *Med.* **362**, 2360–2369 (2010).

486 4. J. Jorba, *et al.*, Update on Vaccine-Derived Poliovirus Outbreaks — Worldwide, January 2018–
487 June 2019. *Morb. Mortal. Wkly. Rep.*, 1024–1028 (2049).

488 5. M. Alleman, *et al.*, Update on Vaccine-Derived Poliovirus Outbreaks - Worldwide July 2019-
489 February 2020. *MMWR Morb Mortal Wkly Re*, 89–495 (2020).

490 6. G. R. Macklin, *et al.*, Evolving epidemiology of poliovirus serotype 2 following withdrawal of the
491 type 2 oral poliovirus vaccine. *Science (80-.).*, eaba1238 (2020).

492 7. J. W. Almond, The attenuation of poliovirus neurovirulence. *Annu. Rev. Microbiol.* **41**, 153–180
493 (1987).

494 8. A. B. Sabin, L. R. Boulger, History of Sabin attenuated poliovirus oral live vaccine strains. *J. Biol.*
495 *Stand.* **1**, 115–118 (1973).

496 9. A. Stern, *et al.*, The Evolutionary Pathway to Virulence of an RNA Virus. *Cell* **169**, 35-46.e19
497 (2017).

498 10. M. Famulare, *et al.*, Sabin Vaccine Reversion in the Field: a Comprehensive Analysis of Sabin-Like
499 Poliovirus Isolates in Nigeria. *J. Virol.* **90**, 317–331 (2015).

500 11. O. M. Kew, R. W. Sutter, E. M. de Gourville, W. R. Dowdle, M. A. Pallansch, Vaccine-derived
501 polioviruses and the endgame strategy for global polio eradication. *Annu. Rev. Microbiol.* **59**,
502 587–635 (2005).

503 12. R. J Duintjer Tebbens, *et al.*, Oral Poliovirus Vaccine Evolution and Insights Relevant to Modeling
504 the Risks of Circulating Vaccine-Derived Polioviruses (cVDPVs). *Risk Anal.* **23** (2013).

505 13. A. R. Muzychenko, *et al.*, Coupled mutations in the 5'-untranslated region of the Sabin poliovirus
506 strains during in vivo passages: structural and functional implications. *Virus Res.* **21**, 111–122
507 (1991).

508 14. K. M. S. de M. Cassemiro, *et al.*, Molecular and Phenotypic Characterization of a Highly Evolved
509 Type 2 Vaccine-Derived Poliovirus Isolated from Seawater in Brazil, 2014. *PLoS One* **11**,
510 e0152251–e0152251 (2016).

511 15. E. A. Simoes, P. Sarnow, An RNA hairpin at the extreme 5' end of the poliovirus RNA
512 genome modulates viral translation in human cells. *J. Virol.* **65**, 913 LP – 921 (1991).

513 16. R. B. Ren, E. G. Moss, V. R. Racaniello, Identification of two determinants that attenuate vaccine-
514 related type 2 poliovirus. *J. Virol.* **65**, 1377–1382 (1991).

515 17. H. Asghar, *et al.*, Environmental Surveillance for Polioviruses in the Global Polio Eradication
516 Initiative. *J. Infect. Dis.* **210**, S294–S303 (2014).

517 18. R. Abraham, P. Minor, G. Dunn, J. F. Modlin, P. L. Ogra, Shedding of Virulent Poliovirus Revertants
518 during Immunization with Oral Poliovirus Vaccine after Prior Immunization with Inactivated Polio
519 Vaccine. *J. Infect. Dis.* **168**, 1105–1109 (1993).

520 19. I. M. Blake, *et al.*, Type 2 Poliovirus Detection after Global Withdrawal of Trivalent Oral Vaccine.
521 *N. Engl. J. Med.* **379**, 834–845 (2018).

522 20. M. Taniuchi, *et al.*, Community transmission of type 2 poliovirus after cessation of trivalent oral
523 polio vaccine in Bangladesh: an open-label cluster-randomised trial and modelling study. *Lancet.*
524 *Infect. Dis.* **17**, 1069–1079 (2017).

525 21. M. Famulare, *et al.*, Community structure mediates Sabin 2 polio vaccine virus transmission.
526 *medRxiv*, 2020.07.01.20144501 (2020).

527 22. M. Famulare, C. Selinger, K. A. McCarthy, P. A. Eckhoff, G. Chabot-Couture, Assessing the stability
528 of polio eradication after the withdrawal of oral polio vaccine. *PLOS Biol.* **16**, e2002468 (2018).

529 23. S. Wassilak, *et al.*, Outbreak of type 2 vaccine-derived poliovirus in Nigeria: emergence and
530 widespread circulation in an underimmunized population. *J. Infect. Dis.* **203**, 898–909 (2011).

531 24. K. M. Thompson, R. J. Duintjer Tebbens, Modeling the dynamics of oral poliovirus vaccine
532 cessation. *J. Infect. Dis.* **210 Suppl**, S475-84 (2014).

533 25. A. L. Hughes, Near-Neutrality: the Leading Edge of the Neutral Theory of Molecular Evolution.
534 *Ann N Y Acad Sci* **1133**, 162–179 (2008).

535 26. L. Chao, Fitness of RNA virus decreased by Muller's ratchet. *Nature* **348**, 454–455 (1990).

536 27. T. Leitner, The Puzzle of HIV Neutral and Selective Evolution. *Mol. Biol. Evol.* **35**, 1355–1358
537 (2018).

538 28. Y. Xiao, *et al.*, RNA Recombination Enhances Adaptability and Is Required for Virus Spread and
539 Virulence. *Cell Host Microbe* **19**, 493–503 (2016).

540 29. O. Tenaillon, The Utility of Fisher's Geometric Model in Evolutionary Genetics. *Annu. Rev. Ecol.*
541 *Evol. Syst.* **45**, 179–201 (2014).

542 30. D. L. Hartl, C. H. Taubes, Towards a theory of evolutionary adaptation. *Genetica* **102–103**, 525–
543 533 (1998).

544 31. J. T. McCrone, *et al.*, Stochastic processes constrain the within and between host evolution of
545 influenza virus. *Elife* **7**, e35962 (2018).

546 32. K. A. McCarthy, G. Chabot-Couture, M. Famulare, H. M. Lyons, L. D. Mercer, The risk of type 2
547 oral polio vaccine use in post-cessation outbreak response. *BMC Med.* **15**, 175 (2017).

548 33. Geneva: World Health Organization, "Strategy for the Response to Type 2 Circulating Vaccine-
549 Derived Poliovirus 2020–2021: An addendum to the Polio Endgame Strategy 2019-2023" (2020).

550 34. Y. Wang, *et al.*, Multipathway Quantitative Assessment of Exposure to Fecal Contamination for
551 Young Children in Low-Income Urban Environments in Accra, Ghana: The SaniPath Analytical
552 Approach. *Am. J. Trop. Med. Hyg.* **97**, 1009–1019 (2017).

553 35. K. Zaman, *et al.*, Can cholera 'hotspots' be converted to cholera 'coldspots' in cholera endemic
554 countries? The Matlab, Bangladesh experience. *Int. J. Infect. Dis.* **95**, 28–31 (2020).

555 36. T. Yates, J. Allen, M. L. Joseph, D. Lantagne, "Short-term WASH interventions in emergency
556 responses in low- and middle-income countries" (2017).

557 37. A. Ramesh, K. Blanchet, J. H. J. Ensink, B. Roberts, Evidence on the Effectiveness of Water,
558 Sanitation, and Hygiene (WASH) Interventions on Health Outcomes in Humanitarian Crises: A
559 Systematic Review. *PLoS One* **10**, e0124688–e0124688 (2015).

560 38. M. Wolfe, M. Kaur, T. Yates, M. Woodin, D. Lantagne, A Systematic Review and Meta-Analysis of
561 the Association between Water, Sanitation, and Hygiene Exposures and Cholera in Case–Control
562 Studies. *Am. J. Trop. Med. Hyg.* **99**, 534–545 (2018).

563 39. P. Van Damme, *et al.*, The safety and immunogenicity of two novel live attenuated monovalent
564 (serotype 2) oral poliovirus vaccines in healthy adults: a double-blind, single-centre phase 1
565 study. *Lancet* **394**, 148–158 (2019).

566 40. J. Breuer, Molecular Genetic Insights Into Varicella Zoster Virus (VZV), the vOka Vaccine Strain,
567 and the Pathogenesis of Latency and Reactivation. *J. Infect. Dis.* **218**, S75–S80 (2018).

568 41. R. C. Edgar, MUSCLE: a multiple sequence alignment method with reduced time and space
569 complexity. *BMC Bioinformatics* **5**, 113 (2004).

570 42. A. Stamatakis, RAxML version 8: a tool for phylogenetic analysis and post-analysis of large
571 phylogenies. *Bioinformatics* **30**, 1312–1313 (2014).

572 43. M. Bessaud, M.-L. Joffret, B. Blondel, F. Delpeyroux, Exchanges of genomic domains between
573 poliovirus and other cocirculating species C enteroviruses reveal a high degree of plasticity. *Sci.*
574 *Rep.* **6**, 38831 (2016).

575 44. E. Svensson, R. Calsbeek, *The Adaptive Landscape in Evolutionary Biology* (OUP Oxford, 2012).

576

577

578

579

580

581

582

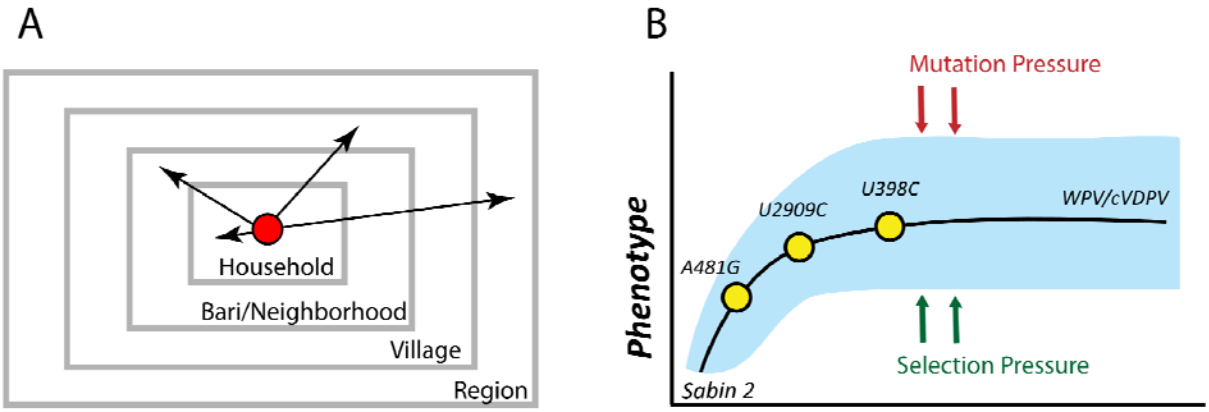

583

584 **Figure 1 Sabin 2 transmission and reversion schematic A**) Multiscale epidemiology model. Individuals
585 are organized into a series of nested, demographic scales defined by households, *baris*/neighborhoods,
586 and villages that together define the greater region. The *bari* is an intergenerational living arrangement
587 of closely related individuals specific to Matlab, the study population the epidemiology model was
588 calibrated to. Conceptually, it is analogous to a neighborhood. Infectious contacts occur at different
589 rates to individuals in each of these demographic scales. During each infectious contact, infected
590 individuals transmit a viral dose that depends on their individual viral shedding concentration and the
591 average fecal oral dose per contact in the population. **B**) Sabin 2 reversion model. Sabin 2 evolution is
592 modeled as a population of competing viral lineages whose average phenotypic end state distribution is
593 identical to that of WPV. Reversion is driven by the acquisition of three gatekeeper mutations (A481G,
594 U2909C, U398C) and the acquisition of deleterious mutations introduced through mutation and purged
595 through selection.

596

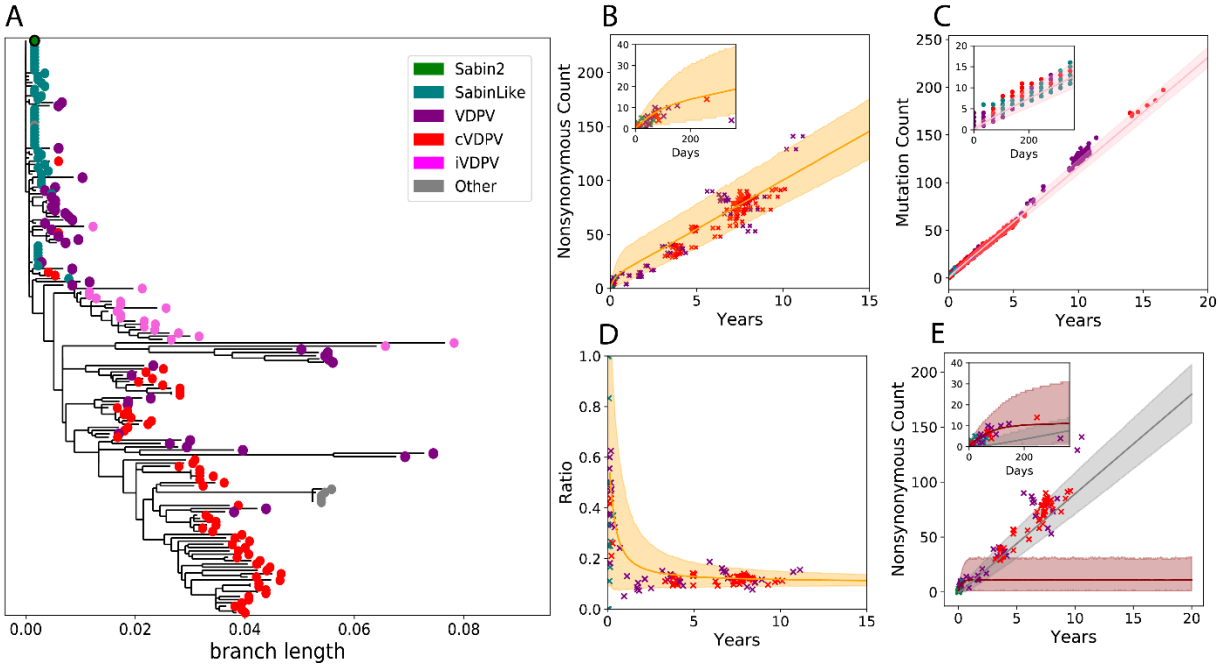

597

598 **Figure 2 Molecular evolution**. **A**) Phylogenetic tree based on the nonsynonymous mutations from the
599 177 whole genome sequences used to calibrate our model. Samples were categorized as Sabin 2, Sabin-
600 Like, vaccine-derived poliovirus isolated from immunocompromised individuals (iVDPV), vaccine-derived
601 poliovirus (VDPV), and cVDPV2. The other category includes the Lansing and MEF-1 laboratory strains as
602 well as several engineered strains derived from the Lansing strain. Samples classified as iVDPV or
603 "other" were excluded from model calibration. **B**) Simulated genome-wide nonsynonymous mutation
604 accumulation over time (*orange*) compared against those observed in the Sabin 2, Sabin-Like, VDPV, and
605 cVDPV2 whole genome sequences. **C**) Simulated (*pink*) VP1 mutation (synonymous and
606 nonsynonymous) accumulation over time compared against the mutation counts observed in 1,643 VP1
607 segments. **D**) The ratio of nonsynonymous and synonymous mutations throughout the genome over
608 time. **E**) Simulated genome-wide nonsynonymous counts partitioned into deleterious (*brown*) and
609 neutral (*grey*). Across all figures, the solid line is the mean simulation outcome and the shaded area
610 marks the boundaries of the middle 95%. Empirical data is represented by points and colored according
611 to the legend in panel **A**. Time was calculated by dividing the number of synonymous mutations per
612 sample by the synonymous substitution rate (3.16E-05 substitutions/bp/day). The insets in **B,C,** and **E**
613 are close ups of the first year of evolution to better show short-term evolution dynamics.

614

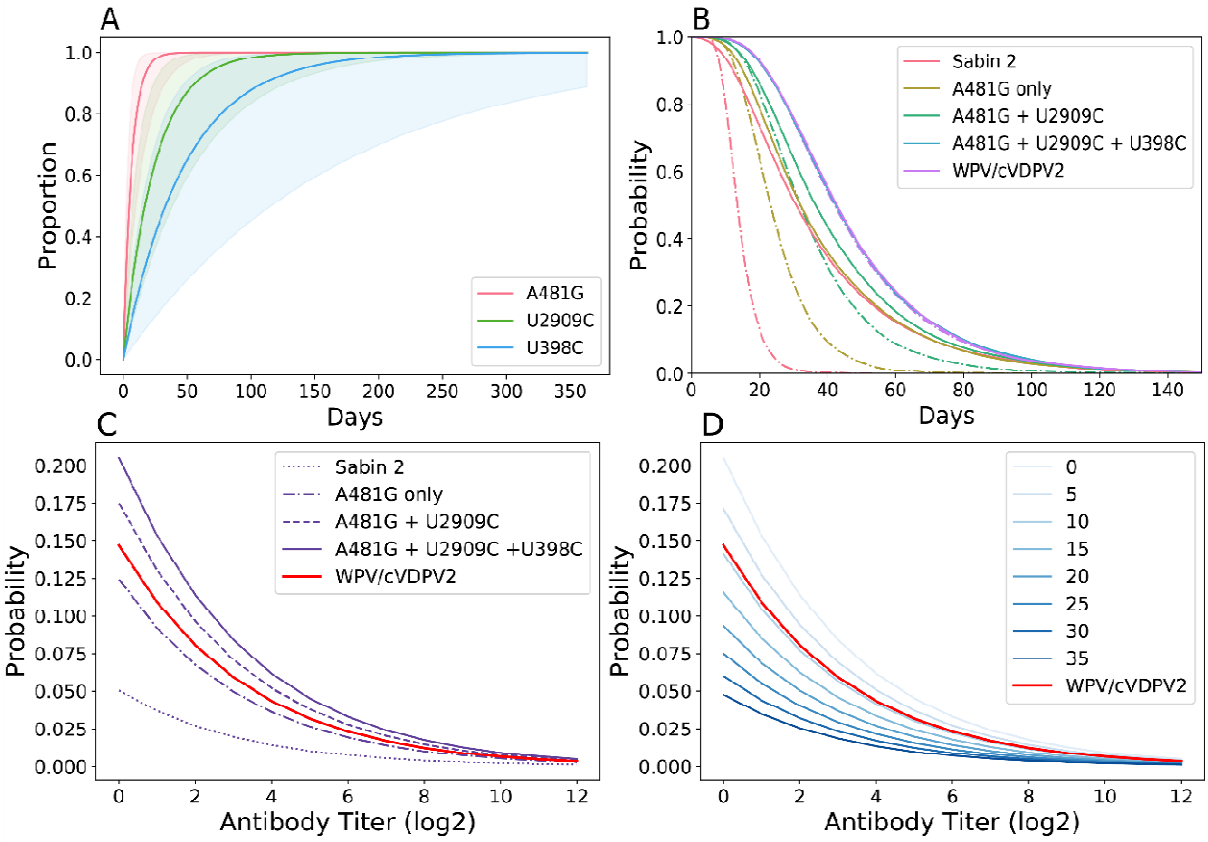

Figure 3 Phenotypic Evolution A) Cumulative density reversion probability functions for the three gatekeeper mutations. The solid line is the mean and the shading the 95% confidence interval. **B)** Shedding duration profile of immunologically naïve individuals infected with Sabin 2, WPV/cVDPV2, and three different intermediate viral genotypes. The dotted lines are the shedding durations of the initial viral genotype assuming no further reversion or evolution. The solid line are the shedding durations of each viral genotype where the reversion of new gatekeeper mutations extends the current shedding duration. Nonsynonymous mutations have no discernable phenotypic effect with regards to shedding duration. **C and D**) Viral infectiousness. Each curve shows strain-specific probability of infection given a single CCID50 dose plotted against immunity. Panel **C** shows infectiousness following the acquisition of each of the three gatekeeper mutations. Panel **D** emphasizes the role of deleterious nonsynonymous

626 mutation and shows the infection probability of different viral genotypes with all gatekeeper mutations

627 and deleterious nonsynonymous mutations count ranging from zero to 35.

628

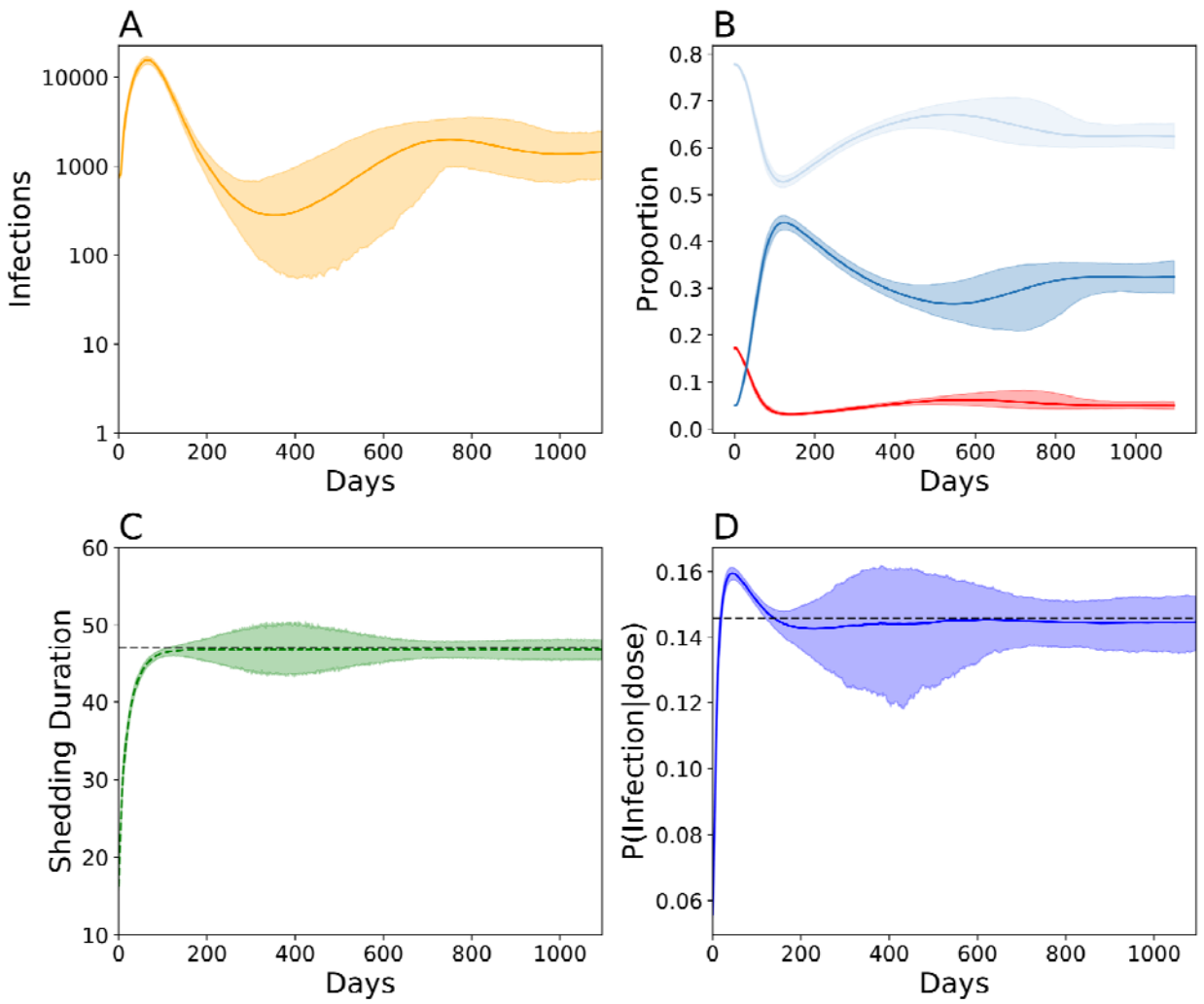

629

630 **Figure 4 Evo-epidemiological dynamics** following a mass vaccination campaign targeting 10% of children

631 under five, five years post-vaccination cessation in Matlab, Bangladesh. Simulations assume 10x the

632 fecal oral dose in Matlab to ensure stable transmission and conditioned on stable, endemic transmission

633 for at least three years. **A**) Total number of infected individuals over time. Solid line indicates the mean

634 and the shading the boundaries of the middle 95% from 200 simulations **B**) Longitudinal immune

profiles for individuals with low immunity (*red*, antibody titer < 8), intermediate immunity (*light blue*, antibody titer > 8 and < 256), and high immunity (*dark blue*, antibody titer > 256). **C**) Shedding duration evolution in naïve individuals over time. **D**) Viral infectiousness evolution over time. For panels **B-D**, the solid line denotes the simulated average and the boundaries the 95% confidence interval around the mean. For panels **C** and **D**, the dashed black line indicates the average WPV phenotype.

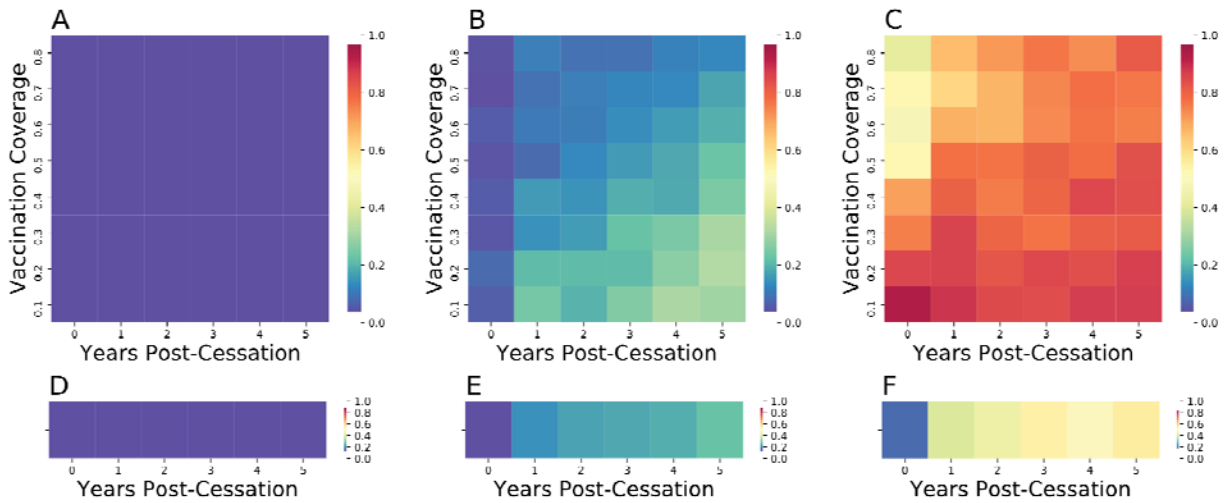

Figure 5 cVDPV2 outbreak risk. cVDPV2 emergence after a mOPV2 vaccination campaign (**A-C**) or importation of a single infant immunized with Sabin 2 (**D-F**) occurring after up to five years of vaccination cessation with fecal-oral doses equivalent to (**A/D**), five times greater (**B/E**), and 10 times greater (**C/F**) than that inferred for Matlab during an mOPV2 clinical trial.

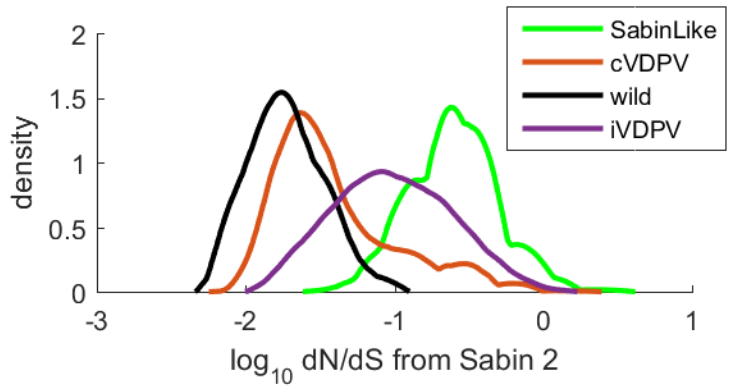

Supplemental Figure 1 dN/dS ratios for Sabin 2-like, cVDPV2, WPV, and iVDPVs.

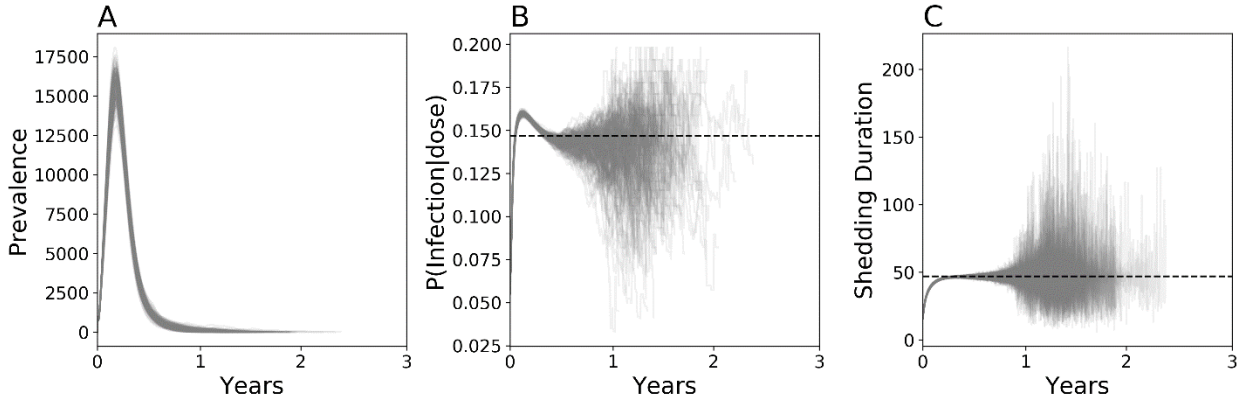

Supplemental Figure 2 Simulated evolutionary and epidemiology dynamics following a mass vaccination campaign targeting 10% of children under five, five years post-vaccination cessation in Matlab, Bangladesh, conditioned on epidemic extinction within the first three years of transmission. **A**) Total number of infected individuals over time **B**) Infectiousness represented as the probability of infecting an immunologically naïve individual given single CCID50 unit dose. **C**) Shedding duration in immunologically naïve individuals. Each line represents a different simulation outcome.

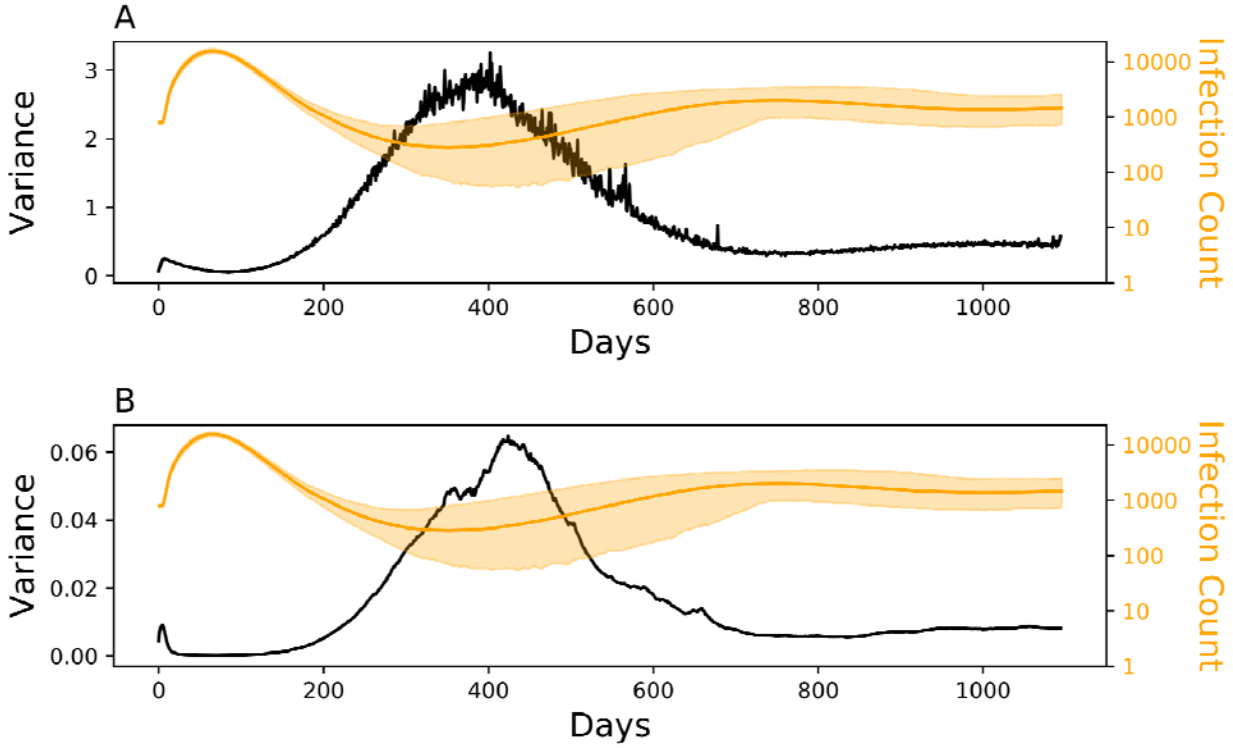

Supplemental Figure 3 The variance of the expected mean (*black*) for shedding duration (**A**) and infectiousness (**B**) compared against infection count (*orange*). The solid orange line is the mean and shading the boundaries of the middle 95 percentile from 200 simulations and identical to **Figure 4A**.

Algorithm 1: Sabin 2 Intra-Host Molecular evolution

```
Initialization:

Step 1: Set reversion times for unreverted gateway mutations
 for mutation in A481G, U2909C, U398C do
    if not reverted then
       Draw reversion time, t_reversion_mutation, from Exponential(λ_mutation)
    end
end

Step 2: Set substitution times for non-gateway mutations
 for mutation in nonsyn_del, nonsyn_neutral, syn do
    Draw substitution time, t_subtitution_mutation, from Exponential(λ_mutation)
end

Step 3: Set recombination time
 Draw recombination time, t_recomb, from Exponential(λ_recomb)

Intra-host Evolution:

while t_infection < t_shed do

    Step 1: Check if unreverted gateway mutations will revert
     for mutation in A481G, U2909C, U398C do
        if t_infection = t_reversion_mutation then
           Revert mutation
        end
    end

    Step 2: Check if new non-gateway mutations are fixed
     for mutation in nonsyn_del, nonsyn_neutral, syn do
        if t_infection = t_reversion_mutation then
           Increase mutation count, n_mutation, by 1
           Draw a new t_mutation from Exponential(λ_mutation)
    end

    Step 3: Check if deleterious nonsynonymous mutations are purged
     if t_infection = t_recomb then
        Draw X from Uniform(0, n_nonsyn_del)
        Subtract X from the deleterious nonsynonymous mutation count, n_nonsyn_del
        Draw a new t_recomb from Exponential(λ_recomb)
end
```

1

Supplemental Figure 4 Pseudocode for simulating Sabin 2 molecular evolution

666

Genotype	Proportion	Expected Shedding Duration
Sabin 2 (no reversions)	0.076 (0.059, 0.093)	14.39 (14.08, 14.69)
A481G only	0.186 (0.162, 0.211)	25.46 (24.71, 26.24)
U2909C only	0.024 (0.014, 0.034)	20.39 (19.85, 20.92)
U398C only	0.01 (0.004, 0.016)	18.98 (18.52, 19.47)
A481G + U398C	0.075 (0.059, 0.091)	33.53 (32.46, 34.62)
U398C + U2909C	0.005 (0.001, 0.01)	26.90 (26.10, 27.72)
A481G + U2909C	0.273 (0.247, 0.300)	36.08 (34.93, 37.26)
A481G + U2909C + U398C	0.352 (0.325, 0.382)	47.51 (45.93, 49.174)

667

668 **Supplemental Table 1** Final viral genotypes in primary vaccine recipients and the expected shedding
669 durations of individuals infected with these genotypes, assuming no further reversion. Bootstrapped
670 confidence interval for the mean were calculated from 1000 simulated primary vaccinations, repeated
671 1000 times. Shedding durations are reported in days. Sabin 2 in this table is defined as a viral genotype
672 with zero gatekeeper reversions.

673

674 **Supplemental File 1** Accession numbers and study origins of the whole genome sequences

675 **Supplemental File 2** Accession numbers and study origins of the VP1 segments

676